Available online at www.sciencedirect.com
SCIENCE DIRECT
ELSEVIER
Journal of the European Ceramic Society 26 (2006) 449–454
ECERS
www.elsevier.com/locate/jeurceramsoc

Graded porous TiO_2 membranes for microfiltration

Wilhelm A. Meulenberg *, Josef Mertens, Martin Bram, Hans-Peter Buchkremer, Detlef Stöver

Forschungszentrum Jülich GmbH, Institut für Werkstoffe und Verfahren der Energietechnik 1, 52425 Jülich, Germany

Available online 24 August 2005

Abstract

Membrane technology can be integrated into many advanced system concepts for the production of liquid energy carriers and chemicals, for microfiltration, oxygen generation, low-CO_2-emission power generation, hydrogen technology and carbon dioxide capture. Forschungszentrum Jülich has developed a composite membrane consisting of a ceramic TiO_2 membrane with pores in the range of 100 nm deposited on a thin planar metallic substrate made of 316L stainless steel powder. Fabrication of substrate and membrane is described in this paper and the composite structure is characterized. The stainless steel substrate is produced by tape casting, the TiO_2 membrane by wet powder spraying or screen printing. Light microscopy, scanning electron microscopy, EDX and XRD are used to characterize the starting materials and layers. The measurement of air flow rates as a function of the pressure drop is given.

Keywords: Composites; Porosity; Sintering; TiO_2; Membranes

1. Introduction

In the present work, a graded composite membrane was developed, which is preferentially intended for microfiltration devices. Microfiltration is now becoming increasingly popular as the preferred mode for a large variety of filtration applications involving the separation and concentration of particulate suspensions or solutions, the recovery of low molecular weight substances and, in some instances, the recovery of macromolecules such as proteins.[1] The pore diameter of the microfiltration membranes ranges from 0.05 to 10 μm.[2]

The composite membrane developed in this work consists of tape-cast stainless steel (316L) substrate, which is coated with a functional ceramic layer by wet powder spraying (WPS) or screen printing. The functional layer is made of TiO_2 pigments. The main advantage of using pigments as starting material for filtration devices is their narrow particle size distribution leading to a well-defined pore size distribution after sintering. Due to the hybrid design, the advantages of ceramic and metallic membranes are combined in a favorable way. Metal substrates are able to withstand mechanical loads, fast thermocycles and corrosive atmospheres and can be easily joined by welding or brazing. Ceramic coatings enable finer microstructures because submicron ceramic powders are easier to handle than metal powders of the same particle size.[3]

Composite membranes also seem to be promising for integration into advanced system concepts for the production of liquid energy carriers and chemicals, separation of particles from fluids, oxygen generation, low-CO_2-emission power generation and hydrogen technology.[4] Up to now, less interest has been focused on these applications.

2. Experimental

2.1. Manufacturing and starting materials

The graded composite membrane developed at Forschungszentrum Jülich is made of a 316L stainless steel substrate coated with a functional TiO_2 layer. The substrate is produced by tape casting, which is a very cost-effective process due to its high automation potential. A large quantity of substrate can be produced in a short time by continuous casting of a slip from a reservoir onto a polymeric tape as shown in Fig. 1a.

* Corresponding author.
E-mail address: w.a.meulenberg@fz-juelich.de (W.A. Meulenberg).

0955-2219/$ – see front matter © 2005 Elsevier Ltd. All rights reserved.
doi:10.1016/j.jeurceramsoc.2005.06.035

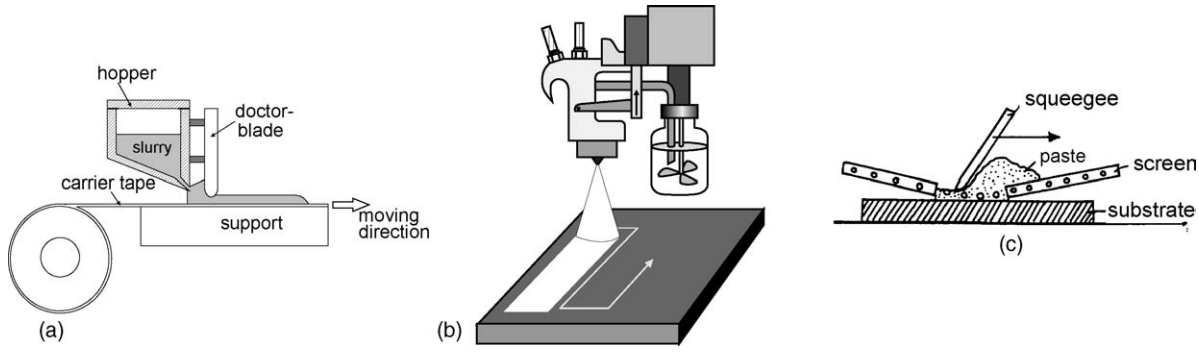

Fig. 1. (a) Substrate manufacturing by tape casting, (b) membrane layer deposition by wet powder spraying and (c) membrane layer deposition by screen printing.

The gap between the doctor blade and the polymeric carrier defines the wet thickness of the tape.[5] As starting material for the 316L substrate gas-atomized metal powders are preferred due to their spherical shape. This particle shape enables an enhanced casting capability and packing density of the green tape. For manufacturing of the substrate a 316L powder from Osprey Metals with a grain size fraction of <5 μm (d_{10} = 2.1 μm, d_{50} = 3.6 μm, d_{90} = 5.9 μm, 80.1% ≤5 μm) was used for all experiments. The chemical composition of the powder is shown in Table 1.

The substrate was manufactured on an FAG 500 tape caster from SAMA Maschinenbau GmbH. For slip production 88 wt.% powder is mixed with 10 wt.% ethanol, a dispersant to stabilize the powder against colloidal forces, a binder (PVB98) to achieve sufficient green strength after drying and to establish the porosity required for the substrate, and a plasticizer to modify the properties of the binder. The slurry was homogenized by mixing it on a rolling bench for 4 h. The slip was cast at a constant speed of 300 mm/min and a width of 300 mm. After drying at room temperature the thickness of the green tape was 500 μm. Then discs with a diameter of 28 mm were punched from the tape. The discs were debindered by annealing at 600 °C for 1 h in an argon atmosphere. The heating and cooling rates of all thermal treatments performed in this investigation were 5 K/min. In order to obtain sufficient green strength for subsequent coating with TiO_2 the samples were pre-sintered for 1 min at 900 °C in vacuum (<10^{-4} mbar). Additionally, a sintering study was performed on uncoated substrates to discover the dependence between the sintering temperature and the porosity. Therefore, sintering was done at 930, 940, 950, 970 and 990 °C in vacuum. The dwell time was 1 h for each sintering temperature.

Table 1
Chemical composition in wt.% of the 316L raw material

Fe	68.76
Cr	16.39
Ni	10.60
Mo	2.1
Mn	1.51
Si	0.53
C	0.078
P	0.025
S	0.007

As starting material for the functional membrane TiO_2 rutile pigments (TRONOX® R-KB-3 from Kerr-McGee Chemical LLC) with a density of 4.1 g/cm^3 were used. The rutile pigments are lattice-stabilized with Al_2O_3. The content of Al_2O_3 is below 5 wt.% and not detectable with XRD (Fig. 2). The particle size of the pigments was d_{10} = 0.03 μm, d_{50} = 0.18 μm, d_{90} = 0.43 μm. The surface area of the powder measured by BET was 15.9 m^2/g.

The functional TiO_2 membrane was applied by wet powder spraying (WPS) and screen printing. For wet powder spraying an ethanol-based suspension containing additions of terpineol, polyethyleneimine (PEI) and acetic acid was used. The content of TRONOX® R-KB-3 powder was 39.8 wt.%. Homogenization was done on a rolling bench for 20 h by adding zirconia milling balls (Ø 3 mm). The viscosity of the suspension was in the range of 0.0035 and 0.0045 Pa s. The suspension was sprayed onto the pre-sintered 316L substrate using a modified spraying gun mounted on a two-axis manipulating system, which principle is shown in Fig. 1b.

A meandering line movement allowed the coating of six samples in one run. The thickness of the coating depends on the spraying parameters. In the present investigation, the parameters were kept constant for all coatings. The operat-

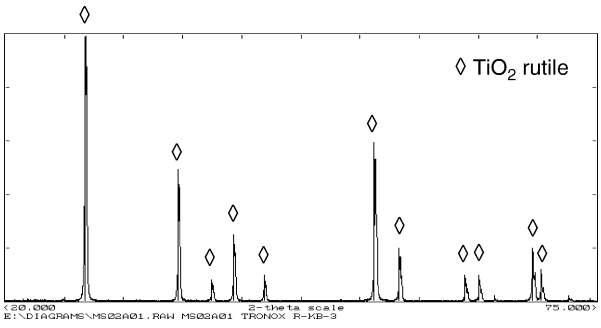

Fig. 2. XRD measurement of the TRONOX® R-KB-3 raw material.

ing speed was 0.125 m/s, the spraying quantity 0.5 g/s, the spraying pressure 0.5 bar and the spraying distance 22 cm. The layer was applied three times so that an overall layer thickness between 40 and 50 μm was expected. After drying at room temperature in a dust-free hood, the samples were debindered and sintered in one run at 950 °C for 1 h in vacuum.

Alternatively, screen printing was used for the deposition of the functional TiO_2 layer (Fig. 1c). A terpineol-based paste with additions of ethylcellulose was used for screen printing. The content of TRONOX® R-KB-3 was 55 wt.%. The paste was homogenized on a three-roller mill. Printing of the paste on the stainless steel substrate was performed on an E1 screen printer from Ekra with a mesh size of 140 μm, a wire diameter of 63 μm, a theoretical paste thickness of 65 μm and an open screen area of 48%. The velocity of the squeegee during printing was 110 mm/s, and the contact distance between sample and mesh was 2 mm. The sintering conditions of the printed samples were corresponded to those of the sprayed samples.

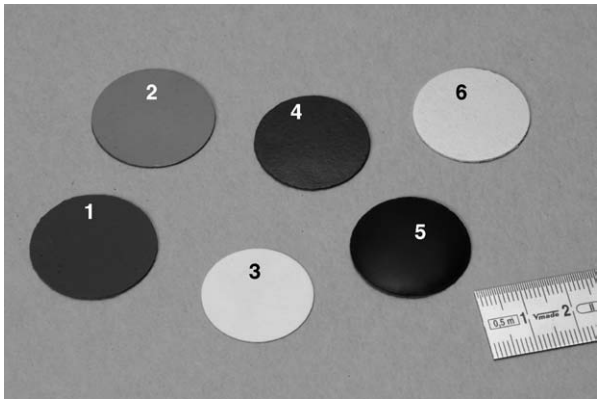

Fig. 3. Photograph of the samples after different manufacturing steps; (1) green 316L substrate, (2) at 900 °C, 1 min pre-sintered 316L substrate, (3) sample 2 with green TiO_2 layer, (4) at 950 °C, 1 h (vacuum) sintered 316L substrate with wet-powder-sprayed TiO_2 layer, (5) at 950 °C, 1 h (vacuum) sintered 316L screen-printed TiO_2 layer, (6) sample 4 after additional heat treatment at 600 °C, 1 h in air.

3. Results and discussion

Fig. 3 shows the samples after the different manufacturing steps. Samples 1 and 2 are uncoated 316L substrates. Samples 3–6 are coated with a TiO_2 layer. After the deposition of the TiO_2 layer the sample has a white color. During sintering in vacuum the color changed into a deep blue. The presumed reason for this effect is given later.

Fig. 4 shows the fractured surface (a) and the surface (b) of the 316L substrate after the pre-sintering process. The homogeneous arrangement of the spherical powder particles is obvious. After pre-sintering, the formation of sintering necks between the powder particles was already observed at the tape surface thus ensuring sufficient strength for subsequent coating.

To find the optimized final sintering temperature sintering experiments are carried out as shown in Fig. 5. The diagram displays a linear relationship between the sintering temperature and the porosity, which allows the adjustment of the porosity of the substrate with a deviation below 3%. The porosity ranges from 30% after sintering at 930 °C to 14% after sintering at 990 °C. At the preferred sintering temperature of the TiO_2 coating (950 °C, 1 h, vacuum) the substrate has a porosity of 24%. The pore size distribution of $d_{10} = 0.44$ μm, $d_{50} = 0.66$ μm and $d_{90} = 1.23$ μm was mainly influenced by the narrow particle size distribution of the starting powder. In Fig. 6, the results of measurements of three samples from different batches are shown. The low deviation demonstrates the good reproducibility of the manufacturing process.

A cross-section of the uncoated substrate sintered at 950 °C is shown in Fig. 7 a. The moderate surface roughness ($R_a = 0.256 \pm 0.008$ μm, $R_{max} = 1.812 \pm 0.226$ μm) and the lack of coarse failures like cracks or pinholes made the substrate suitable for the deposition of a defect-free TiO_2 layer. After sintering, the thickness of the sprayed TiO_2 membrane was in the range of 50 μm as suggested by the spraying parameters (Fig. 7b), while the thickness of the screen-printed TiO_2 layers was 15 μm (not shown here). The SEM pictures in Fig. 8 show the microstructure at the inter-

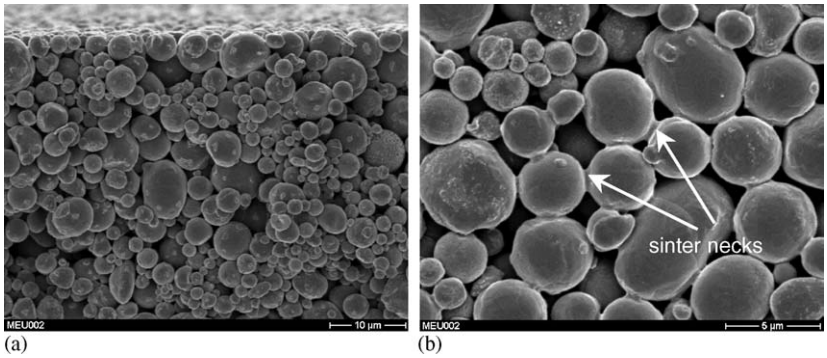

Fig. 4. SEM of the tape-cast 316L substrate after pre sintering at 900 °C, 1 min (a) fractured surface and (b) surface.

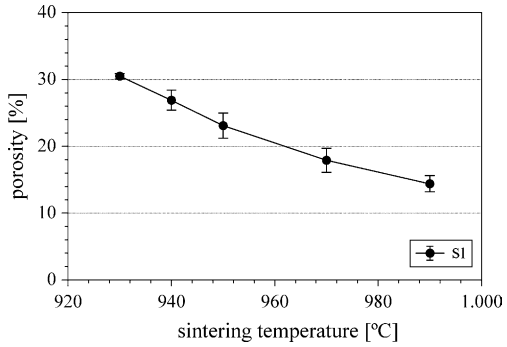

Fig. 5. Porosity as a function of sintering temperature of the 316L substrate, dwell time 1 h in vacuum.

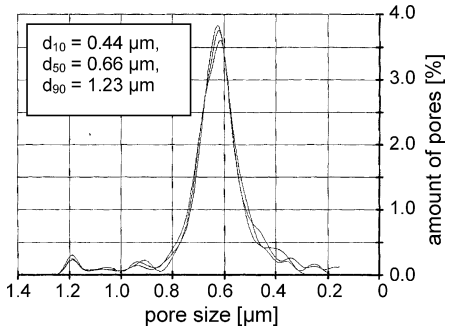

Fig. 6. Pore size distribution of the substrate after sintering at 950 °C, 1 h in vacuum.

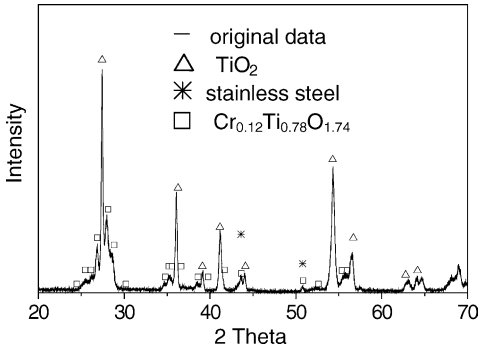

Fig. 9. XRD analysis of the interface between substrate and wet-powder-sprayed functional layer after 950 °C, 1 h in vacuum.

face substrate – sprayed functional layer. The interlocking of both layers is obvious and this enhances the adhesion of the functional layer. Also a diffusion of steel alloying elements into the TiO_2 membrane was observed after the final sintering step. An enrichment of Mn and Cr (markers 1 and 2) in the TiO_2 layer up to a maximum depth of 5 μm was detected by EDX (Fig. 8b). With increasing distance from the interface, pure Ti without traces of the steel alloying elements was found (marker 3). The interdiffusion is coupled with a slight densification of the ceramic membrane. Fig. 9 shows the XRD analysis of the interface. The diffusion of the elements obviously leads to the formation of mixed oxides (e.g. $Cr_{0.12}Ti_{0.78}O_{1.74}$), but TiO_2 rutile still exists as the main

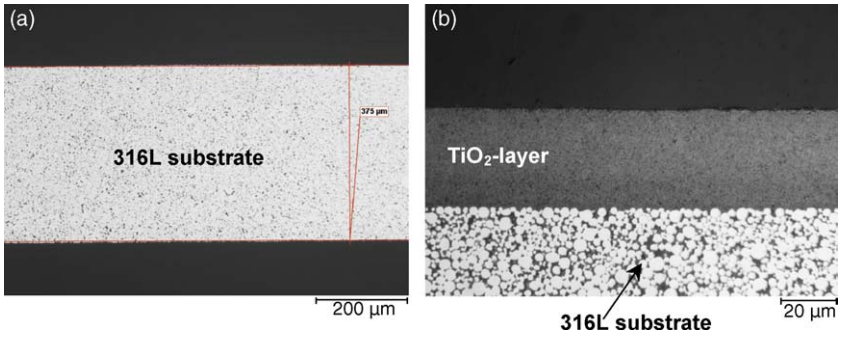

Fig. 7. Cross-section of (a) substrate and (b) the composite after sintering at 950 °C, 1 h, in vacuum.

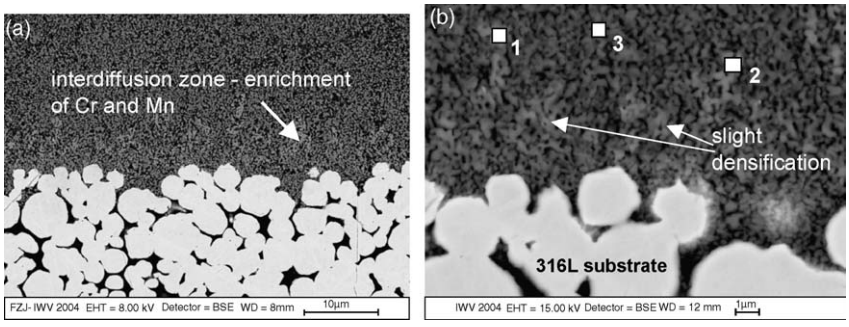

Fig. 8. Cross-section of the interface between substrate and wet-powder-sprayed functional layer after 950 °C, 1 h in vacuum (a) and overview (b) detail, enrichment of Mn and Cr at markers 1 and 2.

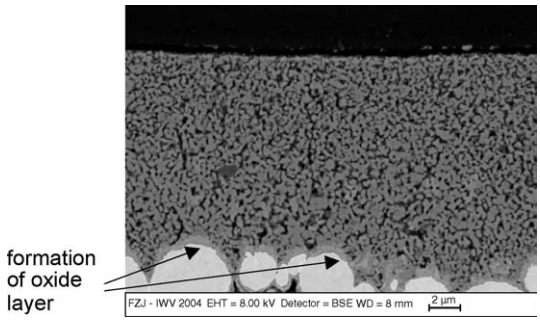

Fig. 10. Composite membrane from Fig. 8 after additional heat treatment at 600 °C, 1 h in air.

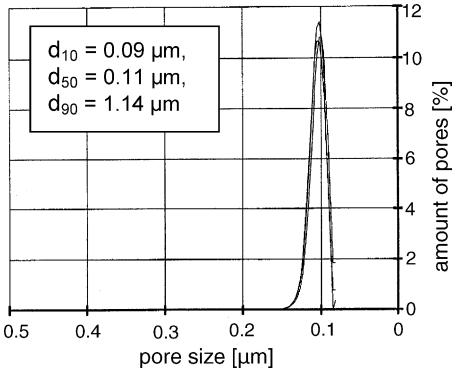

Fig. 12. Pore size distribution of the TiO_2 layer, sintered at 950 °C for 1 h.

phase. No limitations of the application of the membrane due to the formation of mixed oxides not known as yet.

The reduction of the valency of the Ti^{4+} ions is assumed to be the reason for the color change of the membrane. This reduction can be caused by sintering the TiO_2 pigments under reducing atmosphere (vacuum) or by the valency of the Ti ions in the mixed oxide. The first assumption has already been discussed in the literature,[6] where the formation of metastable Ti-oxides, e.g. Ti_4O_7, is described. In our investigations, such metastable phases could not be detected. After an additional thermal treatment at 600 °C in air the color of the TiO_2 membrane changed again into white indicating the reversibility of the effect. As expected, the oxidizing atmosphere leads to the formation of oxides at the surface of the 316L particles (Fig. 10). On a macroscopic scale, some brown dots occurred on the surface of the samples due to this oxidation. In the TiO_2 layer no change of the microstructure is observed so that no influence on the function of the membrane is expected.

Fig. 11 compares the surface of sprayed and screen-printed TiO_2 membranes, both sintered together in one run at 950 °C. Even if the existence of pores in the range of 100 nm is obvious in both cases, the screen-printed layer shows an enhanced homogeneity and sintering density. The higher green density after screen printing is assumed to be the main reason for this behavior.

The related pore size distribution of wet-powder-sprayed samples is shown in Fig. 12. The overlapping lines of the diagram represent the results of measurements on three samples indicating the good reproducibility with an average pore size of $d_{50} = 110$ nm. To evaluate the permeability of each layer of the composite membrane, Fig. 13 compares the air flow rate of an uncoated substrate with the flow rate of the composite membrane made by WPS. The deposition of the TiO_2 membrane decreases the flow rate by a factor of 10 from 2.9×10^6 l/h m^2 bar for the uncoated substrate to

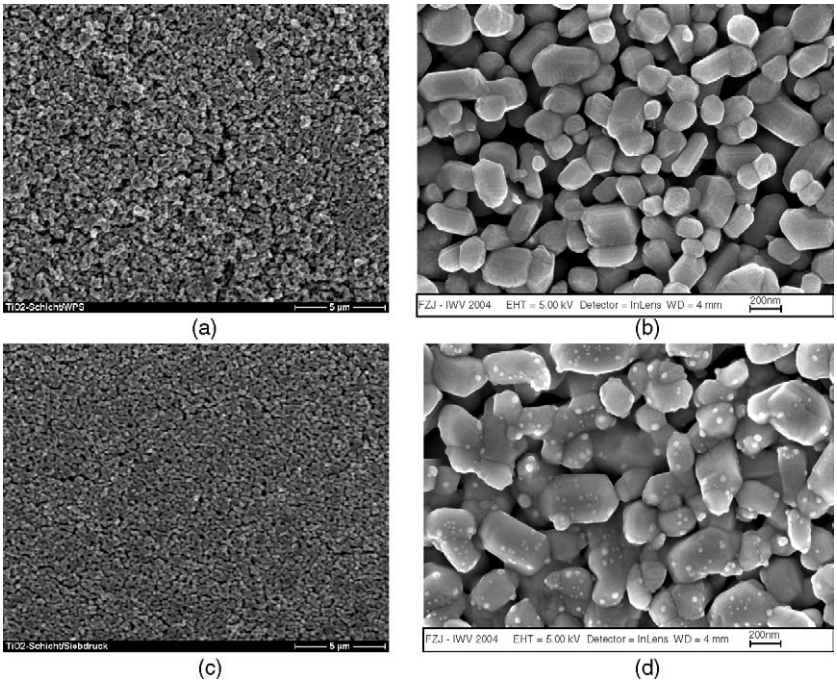

Fig. 11. Surface of the functional TiO_2 layers after 950 °C, 1 h in vacuum (a and b) and wet-powder-sprayed layer (c and d) screen-printed layer.

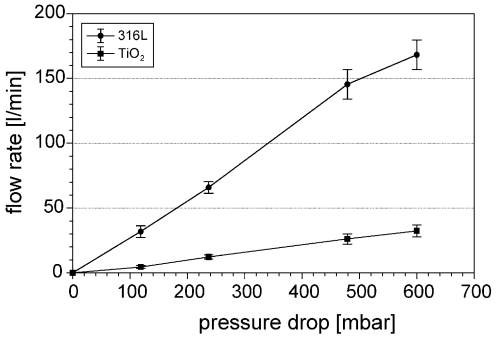

Fig. 13. Comparison of the flow rates of uncoated substrate and composite membrane after sintering at 950 °C, 1 h in vacuum.

1.9×10^5 l/h m^2 bar. It is obvious that the flow rate is mainly influenced by the TiO_2 membrane layer due to the smaller pore size.

4. Conclusion

The combination of metal substrates with functional ceramic coatings makes a new spectrum of applications accessible. In the present work, a composite membrane was developed by the combination of a tape-cast stainless 316L steel substrate followed by wet powder spraying or screen printing of TiO_2 pigments. The porous composite membrane is designed for filtration devices. Apart from the particle size of the starting powder, mainly the sintering temperature determines the properties of the ceramic membrane. Well-grown sintering necks ensure sufficient stability of the porous structure. Optimized sintering temperatures were obtained by pre-sintering the substrate at 900 °C for 1 min, followed by the spraying or printing of TiO_2 pigments and subsequent sintering at 950 °C for 1 h. Post-sintering of the substrate enhances the adhesion of the functional layer exerting compression stresses in the TiO_2 layer. The reproducible pore size distribution of the functional TiO_2 layer with a mean pore diameter of $d_{50} = 0.11$ μm is promising for the desired application. Both manufacturing routes for the functional layers were found to be suitable for producing promising microstructures for filtering applications considering their well-defined pore sizes. While screen printing leads to an enhanced green density resulting in an improved sintering density and surface quality, wet powder spraying seems to be advantageous regarding the adhesion of the functional layer on the substrate, which is caused by a slight penetration of the surface pores of the substrate by the TiO_2 suspension during spraying. After sintering the air flow rate of the composite membrane is 1.9×10^5 l/h m^2 bar. During sintering of the functional layer interdiffusion of alloying elements of the steel in the TiO_2 layer leads to the formation of a new phase (mixed oxide $Cr_{0.12}Ti_{0.78}O_{1.74}$). Up to now, the appearance of the new phase does not appear to influence the application potential. An additional heat treatment in oxidizing atmosphere leads to a corrosion of the 316L particles. No changing of the membrane layer structure could be observed so it is of no relevance for use of the membranes. A longer heat treatment in oxidizing atmosphere at high temperatures could lead to advanced corrosion and destruction of the substrate.

References

1. Katiyar, A., Ji, L., Smirniotis, P and Pinto, N. G., Mesoporous molecular sieves for size selective separation of biomolecules. In *Proceedings of 8th International Conference on Inorganic Membranes*, ed. F. T. Atkin and Y. S. Lin, ISBN 1-929612-67-2, 2004, pp. 63–66.
2. Cheryan, M., *Ultrafiltration and Microfiltration Handbook*. CRC Press, Basel, Switzerland, ISBN 1566765986, 1998.
3. Benfer, S., Árki, P. and Tomandl, G., Ceramic membranes for filtration applications – preparation and characterization. *Adv. Eng. Mat.*, 2004, **6**, 495–500.
4. Mansur, L. K., Bischoff, B. L., Adcock, K.D., Powell, L. E. and Judkins R. R., Nanoporous inorganic membranes for high selectivity hydrogen separations. In *Proceedings of 8th International Conference on Inorganic Membranes*, ed. F. T. Atkin and Y. S. Lin, ISBN 1-929612-67-2, 2004, pp. 167–170.
5. Mistler, R. E. and Twiname, E. R., *Tape Casting – Theory and Practice*. American Ceramic Society, Westerville, OH, USA, ISBN 1-57498-029-7, 2000.
6. Gill, J. A., *Filter element with porous nickel based alloy substrate and metal oxide membrane*, Patent WO 02/26366.